



# To what Extent are $Mg_2$ and $\langle Fe \rangle$ Indicators of Mg and Fe Abundances ?

R. Tantalo<sup>1</sup>, A. Bressan<sup>2</sup>, C. Chiosi<sup>3,1</sup>

<sup>1</sup> Department of Astronomy, Vicolo dell' Osservatorio 5, 35122 Padua, Italy

<sup>2</sup> Astronomical Observatory, Vicolo dell' Osservatorio 5, 35122 Padua, Italy

<sup>3</sup> European Southern Observatory, Karl-Schwarzschild-Strasse 2, D-85748, Garching bei Muenchen, Germany

Received October 1997; accepted

**Abstract.** The gradients in line strength indices such as  $Mg_2$  and  $\langle Fe \rangle$  (Carollo & Danziger 1994a,b; Carollo et al. 1993), and their increase toward massive system (Worthey et al. 1992, Faber et al. 1992, Davies et al. 1993, Weiss et al. 1995) observed in elliptical galaxies are customarily considered as indicators of gradients in the chemical abundances of  $Mg$  and  $Fe$  and arguments are given for an enhancement of  $Mg$  ( $\alpha$ -elements in general) with respect to  $Fe$  toward the center of these galaxies or going from dwarf to massive ellipticals. In this paper, we present a detailed analysis of the whole problem aimed at understanding how the indices  $Mg_2$  and  $\langle Fe \rangle$  depend on the the chemical abundances and age of the stellar mix of a galaxy. We find that  $Mg_2$  and  $\langle Fe \rangle$  do not simply correlate with the abundances of  $Mg$  and  $Fe$  and the ratio  $Mg/Fe$ , but depend also on the underlying distribution of stars in different metallicity bins  $N(Z)$ , or equivalently on the past history of star formation. In practice, inferring the abundance of  $Mg$  and  $Fe$  and their ratio is hampered by the need of some information about  $N(Z)$ . Finally, the observational gradients in  $Mg_2$  and  $\langle Fe \rangle$  do not automatically imply gradients in chemical abundances.

**Key words:** Galaxies: ellipticals – Galaxies: evolution – Galaxies: stellar content – Galaxies: gradients

## 1. Introduction

The line strength indices  $Mg_2$ ,  $\langle Fe \rangle$ ,  $H_\beta$ , etc. and their gradients are customarily used to infer the age and metallicity and their variations across galaxies.

Send offprint requests to: R. Tantalo

Furthermore, in elliptical galaxies, the gradients in  $Mg_2$  and  $\langle Fe \rangle$  have different slopes (Fisher et al. 1995,1996, Carollo & Danziger 1994a,b; Carollo et al. 1993, Davies et al. 1993), which is used as a clue to arguing that  $Mg$  ( $\alpha$ -elements in general) is enhanced with respect to  $Fe$  toward the center.

The bottom line to infer from  $Mg_2$  and  $\langle Fe \rangle$  an enhancement in  $\alpha$ -elements rests on the notion that these two indices depend on age and the abundances of  $Mg$  and  $Fe$ , and that age and abundance effects can somehow be disentangled. If this is the case, the implications are of paramount importance. It is worth recalling that according to the current nucleosynthesis scenario  $Fe$  is mainly produced by Type Ia supernovae (accreting white dwarfs in binary systems in the most popular scheme) and in smaller quantities by Type II supernovae. In contrast, only Type II supernovae contribute to oxygen and  $\alpha$ -elements. Furthermore as the mean lifetime of a binary system (Type Ia progenitors) is  $\geq 1$  Gyr, the contamination by Type I supernovae occurs later as compared to Type II supernovae. Finally, we expect the iron abundance  $[Fe/H]$  and the  $[\alpha/Fe]$  ratios to increase and decrease, respectively, as the galaxy ages. In standard models of galactic chemical evolution, i.e. constant initial mass function and supernova driven galactic winds (cf. Matteucci 1997 for a comprehensive review of the subject), this means that to obtain a galaxy (or region of it) enhanced in  $\alpha$ -elements the time scale of star formation over there must be shorter than about 1 Gyr. This is a very demanding constraint on models of galaxy formation and evolution. It is worth clarifying that such a conclusion is largely independent of the IMF and galactic wind model in usage, even if some *ad hoc* combinations of IMF and/or galactic wind model can be found in which enhancement of  $\alpha$ -elements is possible

irrespective of the argument about the time scale of star formation. The reader is referred to the review article by Matteucci (1997) and the recent study by Chiosi et al. (1997) on an unconventional IMF for more details.

In this paper, we address the question as to what extent the indices  $Mg_2$  and  $\langle Fe \rangle$  (and their gradients) depend on age and chemical abundances, paying particular attention to the complex environment of a galaxy in which stars of many ages and chemical compositions are present. In other words, we seek to clarify how the past history of star formation, which manifests itself in the extant relative distribution of stars per metallicity bin [thereinafter the partition function  $N(Z)$ ], affects the correspondence between indices, ages and abundances.

To this aim, we will utilize the spherical models of elliptical galaxies developed by Tantalo et al. (1997), which take into account gradients in mass density, star formation rate, and chemical abundances (Section 2). With the aid of these models, we predict how the gradients in  $Mg$  and  $Fe$  (and their ratio) translate into gradients in  $Mg_2$  and  $\langle Fe \rangle$ , and check whether a gradient in  $Mg_2$  steeper than a gradient in  $\langle Fe \rangle$  implies an enhancement of  $Mg$  with respect to  $Fe$  toward the center of these galaxies. We anticipate here that, while these models are indeed able to match many key properties of elliptical galaxies, including the gradients in broad band colors (see below), they lead to contradictory results as far as the gradients in line strength indices are concerned (Section 3). To understand the physical cause of this odd behaviour of the models, we check the calibration in use and the response of  $Mg_2$  and  $\langle Fe \rangle$  to chemistry (Section 4). The reason of the contradiction resides in the dependence of the indices in question on the existing  $N(Z)$ , i.e. the past history of star formation. It will be shown that gradients in the indices  $Mg_2$  and  $\langle Fe \rangle$  do not automatically correspond to gradients in the  $Mg$  and  $Fe$  abundances, and their ratios in particular (Section 4). In order to cast more light on this topic, in a way independent of the particular model of galactic evolution, we derive the above indices for single stellar populations (SSP) of different metallicity and age, and look at the possible combinations of these two parameters leading to the same values for the indices (Section 5). Finally, some concluding remarks are drawn in Section 6.

## 2. The reference model

*Sketch of the model.* Elliptical galaxies are supposed to be made of baryonic and dark matter both with spherical distributions but different density profiles. While dark matter is assumed to have remained constant in time, the baryonic material (initially in form of primeval gas) is supposed to have accreted at a suitable rate onto the potential well of the former. The rate at which the density of baryonic material grows with time at any galacto-centric distance is chosen in such a way that at the galaxy age

$T_G$  it matches the radial density distribution derived by Young (1976) for spherical systems. The density profile of the dark-matter is taken from Bertin et al. (1992) and Saglia et al. (1992) however adapted to the Young formalism for the sake of internal consistency. The mass of dark matter is taken in fixed proportions with respect to the luminous one,  $M_D = \theta \times M_L$  (all models below are for  $\theta = 5$ ), Dark matter will only affect the gravitational potential.

Given the total present day luminous mass  $M_L$  of the galaxy (thereinafter in units of  $10^{12} \times M_\odot$  and shortly indicated by  $M_{L,12}$ ) and its effective radius  $R_{L,e}$ , the model is divided into a number of spherical shells, with proper spacing in radius and mass. The luminous mass of each shell is written as

$$\Delta M_{L,S} = \bar{\rho}_L(r) \times \Delta V(r),$$

where  $\Delta V(r)$  is the volume of the shell and  $\bar{\rho}_L(r)$  is the mean density of baryonic material, respectively. The inner and outer radius of each shell are chosen in such a way that, using the Young (1976) tabulations of the mean density as a function of the fractionary radius  $s = r/R_{L,e}$ , the mass  $\Delta M_{L,S}$  amounts to about 5% of the total mass  $M_{L,12}$ . The radial variation of the gravitational potential of dark and luminous mass can be easily derived from the above description. The reader is referred to Tantalo et al. (1997) for all other details.

*Accretion rate.* The collapsing rate of luminous material (gas) is expressed as

$$\left[ \frac{d\rho_L(r, t)}{dt} \right]_{inf} = \rho_{L0}(r) \times \exp\left(-\frac{t}{\tau(r)}\right) \quad (1)$$

where  $\tau(r)$  is the local time scale of gas accretion to be discussed below, and  $\rho_{L0}(r)$  is fixed by imposing that at the present-day age of the galaxy  $T_G$  the density of luminous material in each shell has grown to the value given by the Young profile.

*Star formation rate.* This follows the standard Schmidt law

$$\left[ \frac{d\rho_g(r, t)}{dt} \right]_{sf} = \nu(r) \bar{\rho}_g(r, t) \quad (2)$$

where  $\bar{\rho}_g(r, t)$  is the mean local gas density and  $\nu(r)$  is the specific efficiency of star formation.

*Accretion time scale  $\tau(r)$ .* A successful description of the gas accretion phase is possible adapting to galaxies the radial velocity law describing the final collapse of the core in a massive star (Bethe 1990), i.e. free-fall [ $v(r) \propto r^{-\frac{1}{2}}$ ] in all regions external to a certain value of the radius  $r^*$  and homologous collapse inside [ $v(r) \propto r$ ]. This picture is also confirmed by Tree-SPH dynamical models of elliptical galaxies (cf. Carraro et al. 1997 and references therein).

Let us cast the problem in a general fashion by expressing the velocity  $v(r)$  as

$$v(r) = c_1 \times r^\alpha \quad \text{for } r \leq r^*$$

$$v(r) = c_2 \times r^{-\beta} \quad \text{for } r > r^*$$

(where  $c_1$ ,  $c_2$ ,  $\alpha$  and  $\beta$  are suitable constants), and the time scale of accretion as

$$\tau(r) \propto \frac{r}{v(r)}$$

In the models below we adopt  $\alpha = 2$  (as suggested by the Tree-SPH calculations) and  $\beta = 0.5$  (as indicated by the core collapse analogy). The determination of the constants  $c_1$  and  $c_2$  is not strictly required as long as we seek for scaling relationships.

The time scale of gas accretion can be written as proportional to some arbitrary time scale, modulated by a correction term arising from the scaling law for the radial velocity. For the time scale base-line we can take the free-fall time scale  $t_{ff}$  referred to the whole system,

$$\tau(r) = t_{ff} \times \frac{r^*}{r} \quad \text{if } r \leq r^* \quad (3)$$

$$\tau(r) = t_{ff} \times \left(\frac{r}{r^*}\right)^{3/2} \quad \text{if } r > r^* \quad (4)$$

For the free-fall time scale  $t_{ff}$  we make use of the relation by Arimoto & Yoshii (1987)

$$t_{ff} = 0.0697 \times M_{L,12}^{0.325} \quad \text{Gyr.} \quad (5)$$

Finally, we take  $r^* = \frac{1}{2}R_{L,e}$ . Other choices are obviously possible without changing the overall results of this study.

*Specific efficiency of star formation.* In order to derive the specific efficiency of star formation  $\nu(r)$  we utilize the simple scale relations developed by Arimoto & Yoshii (1987) however adapted to the density formalism. At the typical galactic densities ( $10^{-22}$  -  $10^{-24}$  g cm $^{-3}$ ) and considering hydrogen as the dominant coolant (Silk 1977) the critical Jeans length is much smaller than the galactic radius, therefore the galaxy gas can be considered as made of many cloud lets whose radius is as large as the Jeans scale. If these clouds collapse nearly isothermal without suffering from mutual collisions, they will proceed through subsequent fragmentation processes till opaque small sub-units (stars) will eventually be formed. In such a case the stars are formed on the the free-fall time scale. In contrast, if mutual collisions occur, they will be supersonic giving origin to layers of highly cooled and compressed material, the Jeans scale falls below the thickness of the compressed layer and fragmentation occurs on the free-fall time scale of the high density layers, and finally the whole star forming process is driven by the collision time scale. On the basis of these considerations, we take the ratio

$$\sqrt{\frac{1}{t_{ff} \times t_{col}}} \quad (6)$$

as a measure of the net efficiency of star formation.

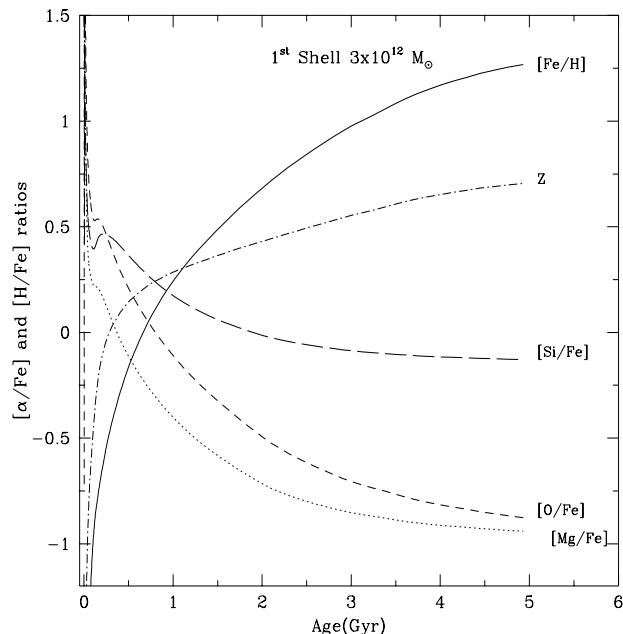


**Fig. 1.** Temporal evolution of four abundance ratios:  $[Fe/H]$  (solid line),  $[Mg/Fe]$  (dotted line),  $[O/Fe]$  (dashed line), and  $[Si/Fe]$  (long-dashed line). The dot-dashed line shows the ratio  $Z/Z_\odot$  as a function of time. The abundance ratios are in the standard notation

Let us express  $\nu(r)$  as the product of a suitable yet arbitrary specific efficiency  $\nu^*$  referred to the whole galaxy and a dimensionless quantity  $F(r)$  describing as the ratio of eq. (6) varies with the galacto-centric distance. An obvious expression for  $F(r)$  is the ratio (6) normalized to its central value.

According to Arimoto and Yoshii (1987) the mean collision time scale referred to the whole galaxy can be expressed as

$$t_{col} = 0.0072 \times M_{L,12}^{0.1} \quad \text{Gyr} \quad (7)$$

With aid of this and the relation for the the free-fall time scale above we can first calculate  $\nu^*$

$$\nu^* = \left[ \sqrt{\frac{1}{t_{ff} \times t_{col}}} \right]_{gal} \quad (8)$$

Extending by analogy the definition of free-fall and collision time scale to each individual region, we get

$$F(r) = \left(\frac{r_c}{r}\right)^{3\gamma} \times \left[ \frac{\bar{\rho}_g(r_c, T_G)}{\bar{\rho}_g(r, T_G)} \right]^\gamma \quad (9)$$

where  $\bar{\rho}_g(r, T_G)$  is the mean gas density within the region of mid radius  $r$  and  $r_c$  is the mid radius of the innermost sphere.

In principle, the exponent  $\gamma$  could be derived from combining the mass dependence of  $t_{ff}$  and  $t_{col}$ , i.e.  $\gamma \simeq 0.2$ . However, the many models calculated by Tantaló et al. (1997) show that in order to recover the observational gradients in broad band colors (and other properties of elliptical galaxies), the efficiency of star formation (i.e.  $F(r)$  in our formulation) must vary with the radial distance more strongly than predicted by  $\gamma = 0.2$ . The following relation is found to give good results

$$\gamma = 0.98 \times M_{L,12}^{0.02} \quad (10)$$

Finally, the total expression for  $\nu(r)$  is

$$\nu(r) = \left[ \frac{1}{t_{ff} \times t_{col}} \right]_{gal}^{0.5} \times \left( \frac{r_c}{r} \right)^{3\gamma} \times \left[ \frac{\bar{\rho}_g(r_c, T_G)}{\bar{\rho}_g(r, T_G)} \right]^\gamma \text{Gyr}^{-1} \quad (11)$$

*Remark.* Before proceeding further, we like to briefly comment on the apparent complexity of the model adopted to perform the analysis. First of all, the model has to be considered as gross tool to understand how gradients in star formation would affect gradients in metallicity and photometric properties. Secondly, the analysis itself is almost model-independent as what matters here is to make use of a reasonably grounded formulation able to predict gradients in chemical abundances and in narrow band indices and look and the mutual correlation between them.

*Galactic winds.* The models allow for galactic winds triggered by the energy deposit from Type I and II supernova explosions and stellar winds from massive stars. The formalism in usage here is the same as in Bressan et al. (1994) and Tantaló et al. (1996) but for two important details: first only a fraction ( $\eta = 0.3$ ) of the kinetic energy by stellar winds is let thermalize, and second the cooling law for supernova remnants is the same as in Gibson (1994, 1996). When the total thermal energy of the gas in each region exceeds the local gravitational potential, gas is supposed to escape from the galaxy and star formation to stop over there.

It worth noticing for the sake of clarity that in presence of galactic winds, the local density and total mass of baryonic material in turn can never reach to the asymptotic values  $\rho_L(r, T_G)$  and  $M_{L,12}$ , respectively. The discussion by Tantaló et al. (1997) of this topic clarifies, however, that the final results of the models are not too severely affected by contradiction between the initial hypothesis (models constrained to match the asymptotic mass) and the real value of this reached in the course of evolution.

*Chemical and photometric evolution.* The chemical evolution of elemental species is governed by the same set of equations as in Tantaló et al. (1996) however adapted to the density formalism and improved as far as the ejecta

and the contribution from Type Ia and Type II supernovae are concerned according to the revision made by Portinari et al. (1997) and Tantaló et al. (1997) to whom we refer. Finally, the line strength indices  $Mg_2$  and  $\langle Fe \rangle$  have been calculated adopting the calibrations by Worthey (1992) and Worthey et al. (1994) as a function of  $[Fe/H]$ ,  $T_{eff}$  and gravity of the stars.

*Mass-radius relationship.* The final step is to adopt a relationship between  $R_{L,e}$  and  $M_L$  so that assigned the total baryonic mass, the effective radius and all other quantities in turn are known. For the purposes of this study and limited to the case of  $H_0 = 50 \text{ Km sec}^{-1} \text{ Mpc}^{-1}$ , we derive from the data of Carollo et al. (1993) and Goudfrooij et al. (1994) the following relation

$$R_{L,e} = 17.13 \times M_{L,12}^{0.557} \quad (12)$$

where  $R_{L,e}$  is in kpc.

*Main results.* This simple modelling of the distribution of density and hence mass in a spherical system allow us to describe the gradients in star formation, chemical abundances, ages, and photometric properties. These models indeed are able to reproduce (i) the slope of colour-magnitude relation by Bower et al. (1992a,b); (ii) the UV excess as measured by the colour (1550–V) by Burstein et al. (1988); (iii) the mass to blue luminosity ratio  $(M/L_B)_\odot$  of elliptical galaxies. See Tantaló et al. (1997) for all other details.

For the purposes of the discussion below, in Table 1 we present the basic data for the central core ( $r = 0.05R_{L,e}$ ) and the first shell ( $0.05 \times R_{L,e} \leq r \leq 0.15 \times R_{L,e}$ ) in a typical galaxy with total luminous mass  $3M_{L,12}$ .

The content of Table 1 is as follows:  $\Delta M_{L,S}$  is the asymptotic luminous mass of the region in units of  $10^{12}M_\odot$ ;  $\nu$  is the local efficiency of the SFR;  $\tau$  is the local time scale of gas accretion in Gyr;  $t_{gw}$  is the age in Gyr at which energy heating by supernova explosions and stellar winds exceeds the local gravitational energy;  $Z_{max}$  and  $\langle Z \rangle$  are the maximum and mean metallicity, respectively;  $G(t)$  and  $S(t)$  are the local fractionary masses of gas and stars gas, respectively, both normalized to the asymptotic mass  $\Delta M_{L,S}$ ;  $N_{enh}$  is the percentage of stars showing  $\alpha$ -enhancement that are present in the region (see below). Finally, in Fig. 1 we show the temporal evolution of the abundances of a few elements in the central core of the model. No detail for the remaining regions is given here but for the gradients in broad band colors and narrow band indices to be presented in Fig. 2 below.

### 3. Casting the gradient contradiction

In Fig. 2 we compare the theoretical and observational gradients in broad-band colors (left panel) and line strength indices (right panel) for our proto-type model. The data are from Carollo & Danziger (1994a,b).

**Table 1.** Basic features for the central core and first shell of the reference model with  $3M_{L,12}$ 

Parameter	Core	1 <sup>st</sup> shell
$\Delta M_{L,S}$	0.146	0.150
$\nu$	7.1	50.0
$\tau$	0.74	0.29
$t_{g\omega}$	5.12	0.79
$Z_{max}$	0.0964	0.0439
$\langle Z \rangle$	0.0365	0.0286
$G(t)$	0.004	0.010
$S(t)$	0.845	0.874
$N_{enh}$	45.7%	53.9%

Remarkably, while the model matches the gradient in broad band colors, it fails as far as the line strength indices  $Mg_2$  and  $\langle Fe \rangle$  and their gradients are concerned. Other cases can be found in the Carollo & Danziger (1994a,b) list (they are not shown here for the sake of brevity), in which either the broad band colors or the line strength indices are matched, but the simultaneous fit of the two sets of data is not possible.

The obvious attitude toward these matters would be to ascribe the above failure to inadequacy of the models (which may certainly be the case) and thus quit the subject. This is a point of embarrassment because there is no obvious explanation as to why models that successfully reproduce many of the observed properties of elliptical galaxies (cf. Bressan et al. 1994, 1996; Tantalo et al. 1996; 1997) fail to match the line strength indices.

In addition to this, and even more relevant to the aims of the present study, a point of contradiction between chemical structure and line strength indices is soon evident. The problem is cast as follows. The theoretical gradients  $[\Delta \ln Mg_2 / \Delta R] \simeq -0.13$  and  $[\Delta \ln \langle Fe \rangle / \Delta R] \simeq -0.11$  (with R the galactocentric distance in kpc) are nearly identical.

This is a surprising result because looking at the data of Table 1 the duration of star formation was much longer in the central core than in the outer shell (the same trend holds for all remaining shells not considered here), which implies that the stars in the core are on the average less  $\alpha$ -enhanced than in the more external regions (cf. the temporal evolution of the elemental abundances shown in Fig. 1), whereas the gradients we have obtained seem to indicate a nearly constant ratio  $[Mg/Fe]$ .

To single out the reason of the contradiction we look at the variation of the abundance ratios  $[Fe/H]$ ,  $[C/Fe]$ ,

$[O/Fe]$ , and  $[Mg/Fe]$  (with respect to the solar value) as a function of the metallicity and time, and the present-day partition function  $N(Z)$ . This allows us to evaluate the fraction of living stars with metallicity above any particular value and with abundance ratios above or below the solar value. The relationships in question are shown in the two panels of Fig. 3 (the left panel is for the central core; the right panel is for the 1<sup>st</sup> more external shell).

In addition to this, we also look at the current age of the stellar population stored in every metallicity bin (we remind the reader that the metallicity in this model is a monotonic increasing function of the age, cf. Fig. 1). The top axis of Fig. 3 shows the correspondence between metallicity and birth-time of the stellar content in each metallicity bin, shortly named single stellar population (SSP). The SSP birth-time is  $t = T_G - T_{SSP}$ , where  $T_G$  is the present-day galaxy age and  $T_{SSP}$  is the current age of the SSP.

From this diagram we learn that the external shell is truly richer in  $\alpha$ -enhanced stars ( $\sim 53.9\%$  of the total) than the central core ( $\sim 45.7\%$  of the total). The percentages  $N_{enh}$  are given in Table 1. This confirms our expectation that the models should predict gradients in line strength indices consistent with the gradients in abundances.

*Which is the reason for such unexpected contradiction?*

One may argue that the above disagreement results either from the adoption of calibrations, such as those by Worthey (1992) and Worthey et al. (1994), which include the dependence on  $[Fe/H]$ ,  $T_{eff}$ , and gravity but neglect the effect of enhancing the  $\alpha$ -elements, or the particular model in usage.

#### 4. Changing calibrations and chemistry

To answer the question posed in the previous section, first we adopt a different calibration in which the effect of  $[Mg/Fe]$  is explicitly taken into account, and second we discuss different, *ad hoc* designed, galactic models in which different levels of enhancement in  $\alpha$ -elements are let occur by artificially changing the history of star formation.

##### 4.1. Calibrations containing $[Mg/Fe]$

Many studies have emphasized that line strength indices depend not only on the stellar parameters  $T_{eff}$  and gravity, but also on the chemical abundances (Barbuy 1994, Idiart et al. 1995, Weiss et al. 1995, Borges et al. 1995).

We start pointing out that in presence of a certain degree of enhancement in  $\alpha$ -elements one has to suitably modify relationship between the total metallicity  $Z$  and the iron content  $[Fe/H]$ . Using the pattern of abun-

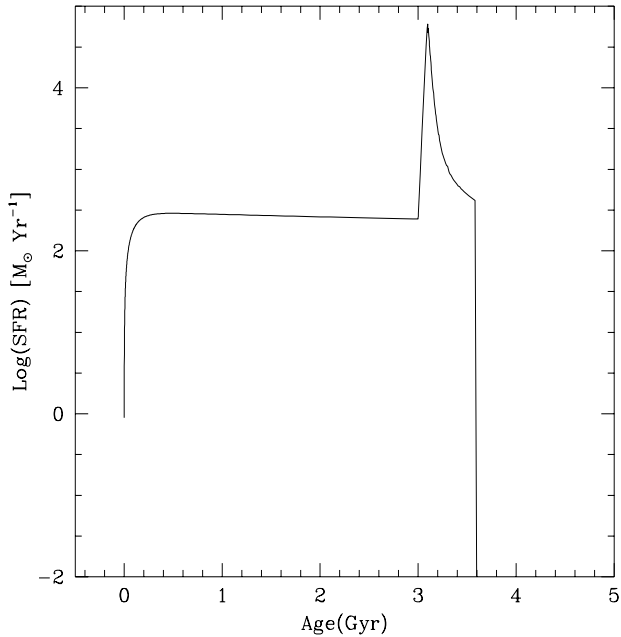


**Fig. 4.** *Model-C*: the star formation rate as a function of the time for the central region of the galaxy model with  $3M_{L,12}$ . At the age of 3 Gyr the efficiency of the SFR is let increase from  $\nu = 0.1$  up to  $\nu = 50$  over a time scale of  $10^8$ yr. The parameters of this model are given in Table 2

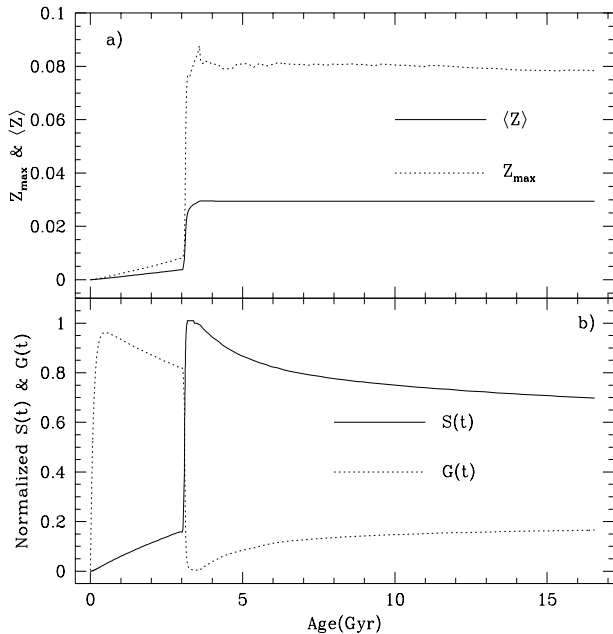


**Fig. 5.** *Model-C*: Panel (a) shows maximum and mean metallicity *dotted* and *solid line*, respectively. Panel (b) shows the fractionary density of gas  $G(t)$  and living stars  $S(t)$  as a function of time, *dotted* and *solid line*, respectively

**Table 2.** Basic properties of the central region of the test models with  $3M_{L,12}$ . Model-A: late galactic wind and no enhancement of  $\alpha$ -elements. Model-B: early galactic wind and enhancement of  $\alpha$ -elements. Model-C: recent burst of star formation, and galactic wind, and strong enhancement of  $\alpha$ -elements

Parameter	Model-A	Model-B	Model-C
$\Delta M_{L,S}$	0.146	0.146	0.146
$\nu$	7.1	100.0	$0.1 \div 50$
$\tau$	0.74	0.05	0.10
$t_{g\omega}$	5.12	0.39	3.58
$Z_{max}$	0.0964	0.0713	0.0878
$\langle Z \rangle$	0.0365	0.0279	0.0294
$G(t)$	0.004	0.002	0.003
$S(t)$	0.845	0.942	0.994
$N_{enh}$	45.7%	85.2%	74.8%

dances by Anders & Grevesse (1989), Grevesse (1991) and Grevesse & Noels (1993), we find the general relation

$$\left[ \frac{Fe}{H} \right] = \log \left( \frac{Z}{Z_{\odot}} \right) - \log \left( \frac{X}{X_{\odot}} \right) - 0.8 \left[ \frac{\alpha}{Fe} \right] - 0.05 \left[ \frac{\alpha}{Fe} \right]^2 \quad (13)$$

where the term  $[\alpha/Fe]$  stand for all  $\alpha$ -elements lumped together.

The recent empirical calibration by Borges et al. (1995) for the  $Mg_2$  index includes the effect of different  $[Mg/Fe]$  ratios

$$\ln Mg_2 = -9.037 + 5.795 \frac{5040}{T_{eff}} + 0.398 \log g +$$

$$0.389 \left[ \frac{Fe}{H} \right] - 0.16 \left[ \frac{Fe}{H} \right]^2 + 0.981 \left[ \frac{Mg}{Fe} \right] \quad (14)$$

which holds for effective temperatures and gravities in the ranges  $3800 < T_{eff} < 6500$  K and  $0.7 < \log g < 4.5$ .

To our knowledge, no corresponding calibration for the  $\langle Fe \rangle$  index is yet available, so that one is forced to adopt that with no dependence on  $[Mg/Fe]$ . Nevertheless, a zero-order evaluation of the effect of  $[Mg/Fe]$  on the  $\langle Fe \rangle$  index is possible via the different relation between  $Z$  and  $[Fe/H]$  of the  $[\alpha/Fe] \neq 0$  case.

The above relations for  $[Fe/H]$ ,  $Mg_2$  and implicitly  $\langle Fe \rangle$  are used to generate new SSPs and galactic models in which not only the chemical abundances are enhanced with respect to the solar value but also the effect of this on the line strength indices is taken into account in a self-consistent manner.

#### 4.2. Three different chemical structures

We present here three galactic models that in virtue of their particular history of star formation, have different chemical structures and degree of enhancement in  $\alpha$ -elements. The discussion is limited to the central region of the  $3M_{L,12}$  galaxy.

*Model-A: late galactic wind.* This case has late galactic wind ( $\sim 5.12$  Gyr), which means that Type Ia supernovae dominate the enrichment in Fe of the gas, and the ratio  $[\alpha/Fe]$  is solar or below solar for most of the time. This model is actually the central region of the  $3M_{L,12}$  galaxy presented above. The percentage ( $N_{enh}$ ) of  $\alpha$ -enhanced stars that are still alive at the age of 15 Gyr amounts to 45.7%.

*Model-B: early galactic wind.* In order to enhance the relative abundance of elements from Type II supernovae we arbitrarily shortened the duration of the star forming period. To this aim, in the central region of the same galaxy, the efficiency of star formation has been increased ( $\nu = 100$ ) and the infall time scale decreases ( $\tau=0.05$  Gyr) so that the galactic wind occurs much earlier than in the previous case (at 0.39 Gyr). The material (gas and stars) of Model-B is therefore strongly enhanced in  $\alpha$ -elements. The percentage ( $N_{enh}$ ) of  $\alpha$ -enhanced stars that are still alive at the age of 15 Gyr amounts to 87.2%.

*Model-C: recent burst of star formation.* A third possibility is considered, in which a burst of star formation can occur within a galaxy that already underwent significant stellar activity and metal enrichment during its previous history. This model (always limited to the central region of the galaxy) has nearly constant star formation rate from the beginning, but at the age (arbitrarily chosen) of 3 Gyr it is supposed to undergo a sudden increase in the star formation rate. To this aim, the specific efficiency of star formation  $\nu$  is let increase from  $\nu = 0.1$  to  $\nu = 50$  over a time scale of  $10^8$  yr. The initial nearly constant stellar activity is secured by adopting a long time scale of gas accretion in the infall scheme ( $\tau = 10$  Gyr). The rate of star formation (in units of  $M_{\odot}\text{yr}^{-1}$ ) as a function of time is shown in Fig. 4. Soon after the intense period of star formation, the galactic wind occurs thus halting star formation and chemical enrichment. The basic chemical properties of the model as a function of the age are shown in Fig. 5. This displays the maximum (*dotted line*) and mean metallicity (*solid line*), and the fractionary mass of gas  $G(t)$  (*dotted line*) and stars  $S(t)$  (*solid line*) both normalized to  $\Delta M_{L,S}$ . The percentage ( $N_{enh}$ ) of  $\alpha$ -enhanced stars that are still alive at the age of 15 Gyr amounts to 74.5%.

The basic data for the three models in question are summarized in Table 2, whereas the evolution of their chemical abundances and present-day partition function  $N(Z)$  are shown in Figs. 6, where the left panel is for

Model-A, the middle panel is for Model-B, and the right panel is for Model-C. These figures are the analog of Fig. 3.

#### 4.3. $Mg_2$ and $\langle Fe \rangle$ in SSPs with $[\alpha/Fe] \neq 0$

To secure full consistency between chemical abundances and line strength indices for the galactic models and make use of the SSP technique (cf. Bressan et al. 1996) one should adopt SSPs with the same pattern of abundances indicated by the chemical models.

To this aim, the distributions of chemical abundances (and their ratios) as a function of the total metallicity and/or time provided by the model galaxies are used to calculate the  $Mg_2$  and  $\langle Fe \rangle$  indices of SSPs with different  $Z$ ,  $[Fe/H]$ ,  $[O/Fe]$ , and  $[Mg/Fe]$ .

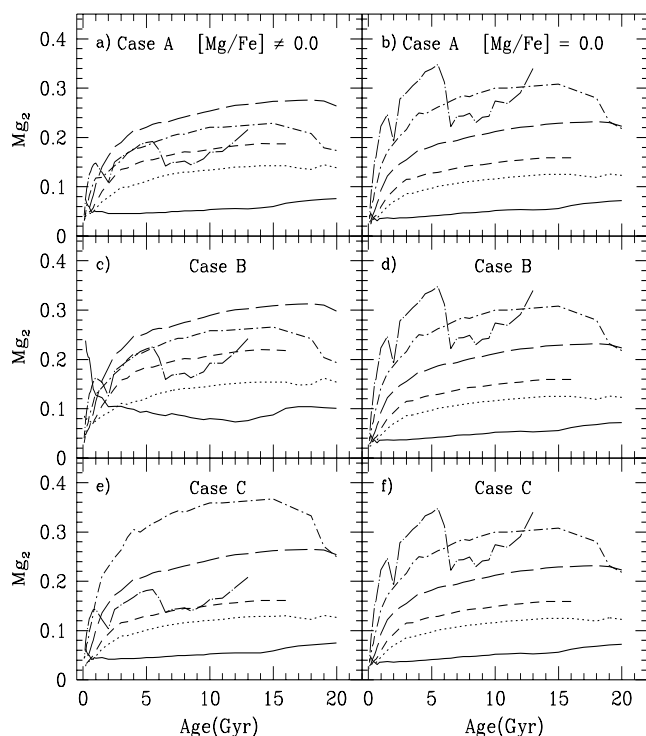


**Fig. 7.** Panels (a), (c) and (e) show the  $Mg_2$  index evolution for SSPs with different metallicity ( $Z=0.0004$ ,  $Z=0.004$ ,  $Z=0.008$ ,  $Z=0.02$ ,  $Z=0.05$  and  $Z=0.1$  *solid dotted dashed long-dashed, dot-dashed and dot-long-dashed lines, respectively*) and the assumption of enhancement in  $\alpha$ -elements. Panels (b), (d) and (f) show the same but without enhancement of  $\alpha$ -elements

To quantify the abundance of  $\alpha$ -elements we prefer to use  $[O/Fe]$  instead of  $[Mg/Fe]$ , because the stellar yields by Portinari et al. (1997) that are at the base of our chemical models somewhat overestimate the production of Fe by Type II supernovae, and underestimate in turn the ratio  $[Mg/Fe]$  as compared to the observational value. Ac-

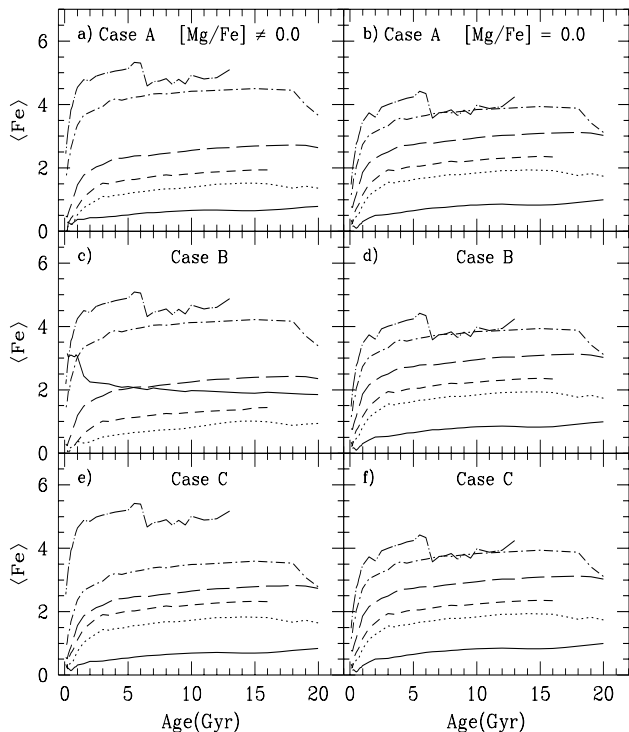


**Fig. 8.** Panels (a), (c) and (e) show the  $\langle Fe \rangle$  index evolution for SSPs with different metallicity ( $Z=0.0004$ ,  $Z=0.004$ ,  $Z=0.008$ ,  $Z=0.02$ ,  $Z=0.05$  and  $Z=0.1$  solid dotted dashed long-dashed, dot-dashed and dot-long-dashed lines, respectively) and the assumption of enhancement in  $\alpha$ -elements. Panels (b), (d) and (f) show the same but without enhancement of  $\alpha$ -elements

According to Portinari et al. (1997) the theoretical  $[Mg/Fe]$  is about  $0.2 \div 0.3$  dex lower than indicated by the observational data. Applying this correction, the ratio  $[Mg/Fe]$  gets close to the ratio  $[O/Fe]$  (see Fig. 6), which somehow justifies our use of  $[O/Fe]$  instead of  $[Mg/Fe]$  in the procedure below. This marginal drawback of the chemical model does not however affect the conclusion of this analysis.

For any value of  $Z$  we read from Fig. 6 the ratios  $[C/Fe]$ ,  $[O/Fe]$ , and  $[Mg/Fe]$ , derive  $[Fe/H]$  from equation (13), and insert  $[Mg/Fe]$ , *i.e.*  $= [O/Fe]$ , and  $[Fe/H]$  into equation (14). It goes without saying that the values of  $[Fe/H]$  derived from Figs. 6 and equation (13) are mutually consistent by definition.

Table 3 shows the values of  $[Fe/H]$  and  $[O/Fe]$  assigned to the SSPs according to the chemical structure of Model-A, Model-B, and Model-C and, for purposes of comparison, to reference SSPs with no enhancement at all.

The temporal evolution of the  $Mg_2$  and  $\langle Fe \rangle$  indices for the SSPs listed in Table 3 is shown in the various panels of Figs. 7 and 8, respectively.

It is soon evident that with  $[\alpha/Fe] = 0$  (right panels of Fig. 7),  $Mg_2$  monotonically increases with the metallicity, but for the extreme SSP with  $Z=0.1$  for which the trend is reversed at ages older than 5 Gyr. When  $[\alpha/Fe] \neq 0$ , the trend is more complicated as it depends on the degree of enhancement. For cases A and B, the strongest  $Mg_2$  happens to occur for  $Z = 0.02$ , whereas for case C it occurs for  $Z = 0.05$  (left panels of Fig. 7).

As far as  $\langle Fe \rangle$  is concerned, with  $[\alpha/Fe] = 0$  the index gets stronger at increasing metallicity but for the extreme case of  $Z = 0.1$ , in which  $\langle Fe \rangle$  gets lower than or comparable to the values for the case with  $Z = 0.05$  at ages older than about 5 Gyr (right panels of Fig. 8). In presence of enhancement in  $\alpha$ -elements, there is a significant dependence of  $\langle Fe \rangle$  on this parameter even at our zero-order evaluation (see the left panels of Fig. 8). Although the exact evaluation of the effect of  $[Mg/Fe]$  on  $\langle Fe \rangle$  is hampered by the lack of the proper calibration, still the above experiments clarify that it cannot be neglected.

#### 4.4. The $Mg_2$ and $\langle Fe \rangle$ indices of galaxies

What the results for the  $Mg_2$  and  $\langle Fe \rangle$  indices would be when applying these SSPs to model galaxies? The situation is displayed in the various panels of Fig. 9 for  $Mg_2$  and Fig. 10 for  $\langle Fe \rangle$ . The combined analysis of the chemical structures, partition functions  $N(Z)$ , and temporal variations of the  $Mg_2$  and  $\langle Fe \rangle$  indices of the model galaxies (Figs. 9 and 10) allow us to make the following remarks:

- (i)  $[Mg/Fe] \neq 0$ :  $Mg_2$  in Model-A (late wind, no chemical enhancement) is always weaker than in Model-B (early wind, significant chemical enhancement). However, the difference is large for ages younger than about 5 Gyr, and gets very small up to vanishing for older ages.  $Mg_2$  of Model-C is always weaker than Model-A and Model-B which means that the higher (or comparable) enhancement in  $\alpha$ -elements of Model-C with respect to the previous ones does not produce a stronger  $Mg_2$  index. The age dependence of  $\langle Fe \rangle$  is more intriguing. At young ages ( $< 5$  Gyr) the intensity of  $\langle Fe \rangle$  gets stronger passing from Model-C to Model-A and finally Model-B. At ages older than 5 Gyr, Model-A has the strongest  $\langle Fe \rangle$  whereas Model-B and Model-C are weaker and of the same intensity.
- (ii)  $[Mg/Fe] = 0$ :  $Mg_2$  in Model-A (late wind, no chemical enhancement) is first weaker than in Model-B (early wind, significant chemical enhancement) up to ages of about 5 Gyr, and then becomes significantly stronger at older ages. Finally, the  $Mg_2$  index of Model-C (burst of star formation, and strong enhancement) is weaker or about equal to that of Model-A and Model-B. The index  $\langle Fe \rangle$  closely follows the trend of  $Mg_2$  all over the age range.

It follows that both  $Mg_2$  and  $\langle Fe \rangle$  do not simply correlate with age,  $[Fe/H]$  and  $[Mg/Fe]$ . The striking result



**Table 3.**  $[O/Fe]$  and  $[Fe/H]$  ratios for SSPs with enhancement of  $\alpha$ -elements according to Model-A, Model-B and Model-C. The same ratios for the reference SSPs with no enhancement are also shown

Z	Model-A		Model-B		Model-C		Reference SSPs	
	$[O/Fe]$	$[Fe/H]$	$[O/Fe]$	$[Fe/H]$	$[O/Fe]$	$[Fe/H]$	$[O/Fe]$	$[Fe/H]$
0.0004	+0.8	-2.38	+3.28	-4.87	+0.51	-2.13	0.0	-1.71
0.004	+0.6	-1.22	+1.72	-2.23	+0.14	-0.82	0.0	-0.71
0.008	+0.5	-0.80	+1.22	-1.44	+0.03	-0.42	0.0	-0.39
0.02	+0.4	-0.30	+0.72	-0.57	+0.30	-0.22	0.0	+0.03
0.05	-0.50	+0.88	-0.25	+0.69	+0.31	+0.24	0.0	+0.50
0.1	-0.80	+1.55	-0.59	+1.40	-0.87	+1.60	0.0	+0.95

is that  $Mg_2$  and to some extent  $\langle Fe \rangle$  as well of models with supposedly the highest degree of enhancement in  $\alpha$ -elements happen to be weaker than in those with no enhancement.

*What causes the odd behaviour of  $Mg_2$  and  $\langle Fe \rangle$  as a function of the age and underlying chemical structure of the model galaxy ?*

To answer this question, we have artificially removed from the partition function  $N(Z)$  all the stars in certain metallicity bins and re-calculated the line strength indices for the three models.

Panels (c) and (d) of Figs. 9 and 10 show the results when all stars with metallicity higher than  $Z=0.05$  are removed. This is motivated by the trend as function of the metallicity shown by the SSPs we have already pointed out. The situation remains practically unchanged.

Likewise, panels (e) and (f) of Figs. 9 and 10 show the same but when all stars with metallicity lower than  $Z = 0.008$  are removed. Now the results change significantly. In the case of  $[Mg/Fe] \neq 0$ , the  $Mg_2$  index of Model-B is always much stronger than that of Model-A. In such a case there is correspondence between the strength of the index and the amount of enhancement in  $\alpha$ -elements. In contrast,  $\langle Fe \rangle$  of Model-A is first slightly weaker and then stronger than in Model-B, whereas that of Model-C is first weaker and then almost equal to that of Model-B. cases. In the case of  $[Mg/Fe] = 0$ , at ages older than about 5 Gyr the  $Mg_2$  and  $\langle Fe \rangle$  of the three models are almost equal each other, with a marginal increase passing from Model-C to Model-B and Model-A. At younger ages, while Model-A and Model-C have nearly the same indices, Model-B has always the strongest values.

The above analysis clarifies in a quantitative fashion a number of important clues:

- In galaxies, both  $Mg_2$  and  $\langle Fe \rangle$  depend on the age,  $N(Z)$ ,  $[Fe/H]$ , and  $[Mg/Fe]$  in a somewhat unpredictable fashion.
- Because of this, inferring from the above indices the abundance ratio  $[Mg/Fe]$  and the enhancement of  $\alpha$ -

elements is a difficult task with somewhat ambiguous results.

- Different slopes of the gradients in  $Mg_2$  and  $\langle Fe \rangle$  do not automatically imply gradients in chemical abundances or enhancement ratios.

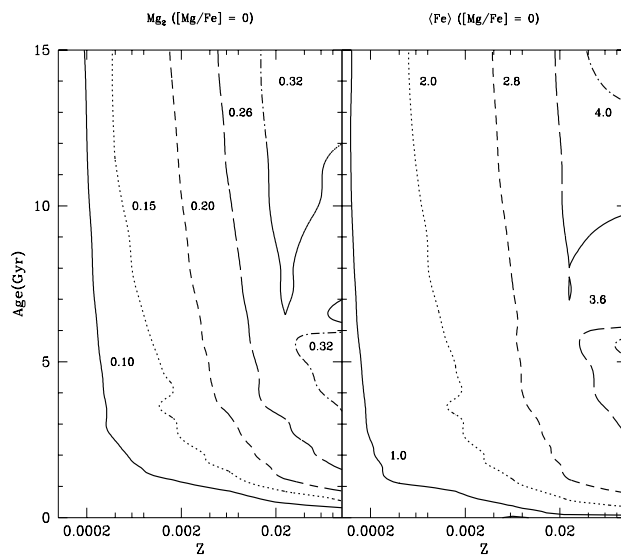


**Fig. 11.** Curves of constant  $Mg_2$  (left) and  $\langle Fe \rangle$  (right) at varying age (in Gyr) and metallicity ( $Z$ ) for SSP with no enhancement in  $\alpha$ -elements. The calibrations in use are from Worthey et al. (1994). The intensity of the indices is annotated along the curves

## 5. Indices in the age-metallicity plane of SSPs

We like to conclude this study presenting the loci of constant  $Mg_2$  and  $\langle Fe \rangle$  in the age-metallicity plane of SSPs.

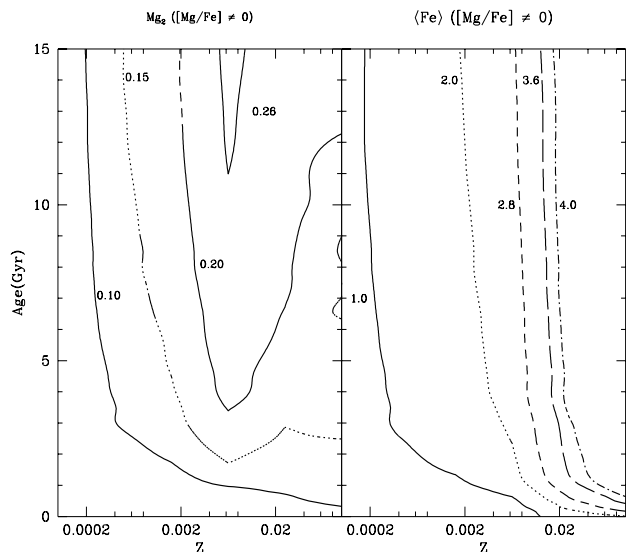


**Fig. 12.** The same as in Fig. 11 but for SSP with enhancement if  $\alpha$ -elements according to the entries of Table 3. The calibrations in use is from Borges et al. (1995) for  $Mg_2$  and Worthey et al. (1994) for  $\langle Fe \rangle$  however corrected for the different relation between  $Z$  and  $[Fe/H]$  in presence of enhancement in  $\alpha$ -elements. The intensity of the indices is annotated along the curves

This is shown in Figs. 11 and 12 displaying the above indices with and without enhancement of  $\alpha$ -elements using the calibrations discussed in the previous sections.

This plane can be used to quickly check how gradients in ages and/or metallicities across galaxies (inferred from other independent analysis) would reflect onto gradients in  $Mg_2$  and  $\langle Fe \rangle$  and vice-versa.

An interesting feature to note, is the marked dip in the  $Mg_2$  index for values greater than a certain limit that occurs at a certain value of the metallicity. The threshold value for  $Mg_2$  is about 0.26 and the metallicity is about 0.03 in the case of no enhancement, whereas they are lowered to 0.15 and 0.008, respectively, in presence of enhancement.

Starting from the observational result that in general elliptical galaxies show stronger  $Mg_2$  and  $\langle Fe \rangle$  toward the center, and representing the local mix of stellar population in a galaxy (center and/or external regions) with a mean SSP of suitable age and composition, we see that the observational gradient in  $Mg_2$  and  $\langle Fe \rangle$  could be compatible with (i) either a nucleus more metal-rich and older than the external regions; (ii) or nucleus more metal-rich and younger than the external regions. In contrast a nucleus less metal-rich and older than the external regions would lead to gradients in  $Mg_2$  and  $\langle Fe \rangle$  oppo-

site to what observed. The situation is straightforward with the Worthey (1992) calibrations, whereas it is somewhat intrigued with the Borges et al. (1995) calibration in presence of  $\alpha$ -enhancement. It worth recalling here that Bressan et al. (1996) analyzing the Gonzales (1993)  $H_\beta$  and  $[Mg/Fe]$  data for elliptical galaxies and their variation across these systems suggested that most galaxies ought to have nuclei with higher metallicities and longer durations of star forming activity than the peripheral regions. This suggestion is fully compatible with the gradients in  $Mg_2$  and  $\langle Fe \rangle$  observed in elliptical galaxies.

## 6. Summary and conclusions

Aim of this study was to ascertain on a quantitative basis the effect of age, metallicity, partition function  $N(Z)$ , abundance ratio  $[Mg/Fe]$ , and calibration in usage on the line strength indices  $Mg_2$  and  $\langle Fe \rangle$  from whose gradients the problem of the possible enhancement of  $\alpha$ -elements toward the center of elliptical galaxies originates. Although by no means we want to exclude such a possibility, the attention is called on a number of indirect effects that could invalidate the one-to-one correlation between the index intensity and the abundance of the corresponding element, and indirectly on the one-to-one correlation between the relative slopes of the observational gradients and the inferred spatial variation of abundance ratios ( $[\alpha/Fe]$  in particular).

The results of this study can be summarized as follows:

1. The intensity of  $Mg_2$  does not simply correlate with the abundance of  $Mg$  and the ratio  $[Mg/Fe]$  in particular.
2. The intensity of  $Mg_2$  does not simply correlate with the age or the metallicity.
3. The intensity of  $Mg_2$  much depends on the partition function  $N(Z)$ .
4. Likewise for the  $\langle Fe \rangle$  index.
5. Inferring the abundance of  $Mg$  or the enhancement ratio  $[Mg/Fe]$  is a cumbersome affair whose solution is not always possible because hints on  $N(Z)$  are needed.
6. The observational gradients in  $Mg_2$  and  $\langle Fe \rangle$  do not automatically imply gradients in the abundances of  $Mg$  and  $Fe$  or enhancement ratios. Inferring from the observational  $Mg_2$  and  $\langle Fe \rangle$  constraints on the past history of star formation (via the different time scales of  $Mg$  and  $Fe$  enrichment) may be risky.

Although most of these conclusions have already been around in literature, their quantitative assessment has never been attempted before in a systematic fashion, in particular in the complex but realistic situation in which many stellar populations with different ages, metallicities, and abundance ratios are present.

*Acknowledgements.* We are most grateful to Dr. Guy Worthey for his constructive referee report which much contributed to improve upon the original manuscript. This study has

been financed by the Italian Ministry of University, Scientific Research and Technology (MURST), the Italian Space Agency (ASI), and the European Community TMR grant #ERBFMRX-CT96-0086.

This article was processed by the author using Springer-Verlag L<sup>A</sup>T<sub>E</sub>X A&A style file L-AA version 3.

## References

- Anders E., & Grevesse N., 1989, *Geochim. Cosmochim. Acta* 53, 197
- Arimoto N., & Yoshii Y., 1987, *A&A* 173, 23
- Barbuy B., 1994, *ApJ* 430, 218
- Bertin G., Saglia R.P., & Stiavelli M., 1992, *ApJ* 411, 153
- Bethe H.A. 1990, *Reviews of Modern Physics*, 62, no. 4, 801
- Borges A.C., Idiart T.P., De Freitas Pacheco J.A., & Thevenin F., 1995, *AJ* 110, 2408
- Bower R.G., Lucey J.R., & Ellis R.S. 1992a, *MNRAS* 254, 589
- Bower R.G., Lucey J.R., & Ellis R.S. 1992b, *MNRAS* 254, 601
- Bressan A., Chiosi C., Fagotto F., 1994, *ApJS* 94, 63
- Bressan A., Chiosi C., Tantalo R., 1996, *A&A* 311, 425
- Burstein D., Bertola F., Buson L., Faber S.M., & Lauer T.R., 1988, *ApJ* 328, 440
- Carollo C.M., Danziger I.J., 1994a, *MNRAS* 270, 523
- Carollo C.M., Danziger I.J., 1994b, *MNRAS* 270, 743
- Carollo C.M., Danziger I.J., Buson L., 1993, *MNRAS* 265, 553
- Carraro G., Lia C., & Chiosi C. 1997, *MNRAS*, submitted
- Davies R.L., Sadler E.M. & Peletier R. 1993, *MNRAS* 262, 650
- Faber S.M., Worthey G., & Gonzales J.J. 1992, in *IAU Symp.* 149, eds. B. Barbuy and A. Renzini, p. 255
- Fisher D., Franx M., Illingworth G. 1996, *ApJ* 459, 110
- Fisher D., Franx M., Illingworth G. 1995, *ApJ* 448, 119
- Gibson B.K., 1994, *MNRAS* 271, L35
- Gibson B.K., 1996, *MNRAS* 278, 829
- Gonzales J.J., 1993, Ph.D. Thesis, University of California, Santa Cruz
- Goudfrooij P., Hansen L, Jorgensen H.E., Norgaard-Nielsen B.H., de Jong T., & van der Hoeck L.B., *A&AS* 104, 179
- Grevesse N., 1991, *A&A* 242, 488
- Grevesse N., Noels A., 1993, *Phys. Scr. T.* 47, 133
- Idiart T.P., de Freitas Pacheco J.A., 1995, *AJ* 109, 2218
- Matteucci F., 1997, *Fundamentals of Cosmic Physics*, in press
- Portinari L., Chiosi C., Marigo P., & Bressan A., 1997, *A&A* submitted
- Saglia R.P., Bertin G., Stiavelli M., 1992, *ApJ* 384, 433
- Silk J., 1977, *ApJ* 214, 243
- Tantalo R., Chiosi C., Bressan A., Fagotto F., 1996, *A&A* 311, 361
- Tantalo R., Chiosi C., Bressan A., Marigo P., Portinari L., 1997, *A&A* submitted
- Young P.J., 1976, *AJ* 81, 807
- Weiss A., Peletier R.F., Matteucci F., 1995, *A&A* 296, 73
- Worthey G., 1992, Oh.D. Thesis, Univ. California, Santa Cruz
- Worthey G., Faber S.M., & Gonzales J.J., 1992, *ApJ* 398, 69
- Worthey G., Faber S.M., Gonzales J.J., Burstein D., 1994, *ApJS* 94, 687

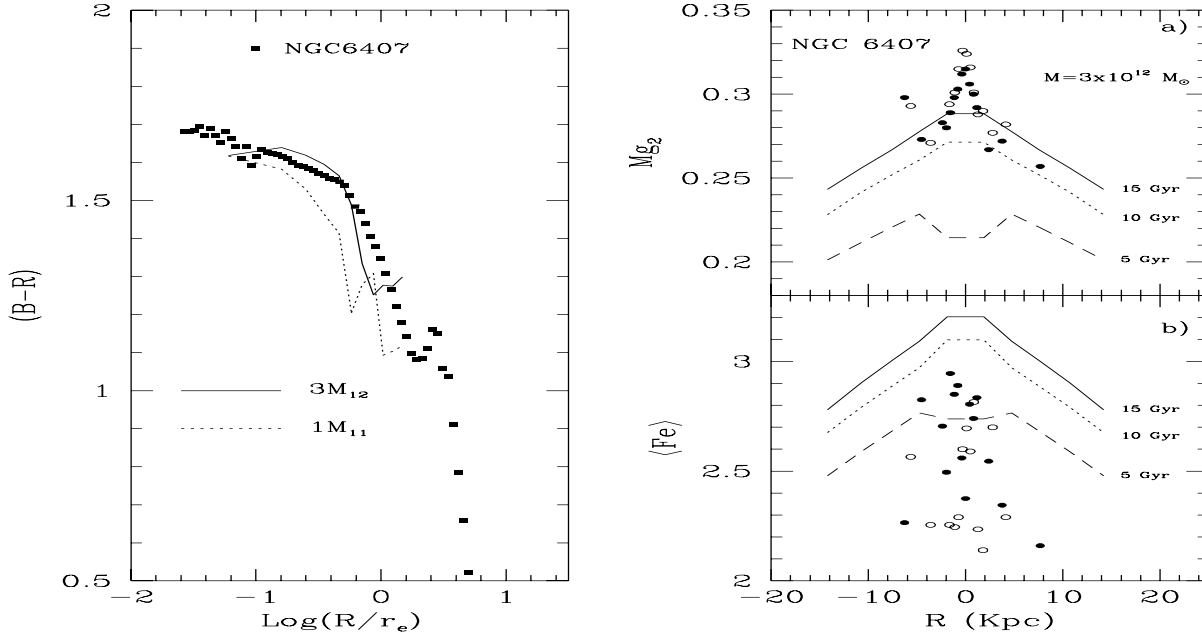


**Fig. 2.** Gradients in colors and line strength indices for the galaxy NGC 6407 (Carollo & Danziger 1994a). *Left Panel:* comparison with the theoretical gradients in  $(B-R)$  for models of different mass and same age (15 Gyr). *Right Panel:* comparison with the theoretical gradients in line strength indices for the  $3 \times M_{L,12}$  model which has nearly the same  $M/L_B$  ratio as NGC 6407. Finally, the observational data along major and minor axis are indicated by full and empty circles, respectively

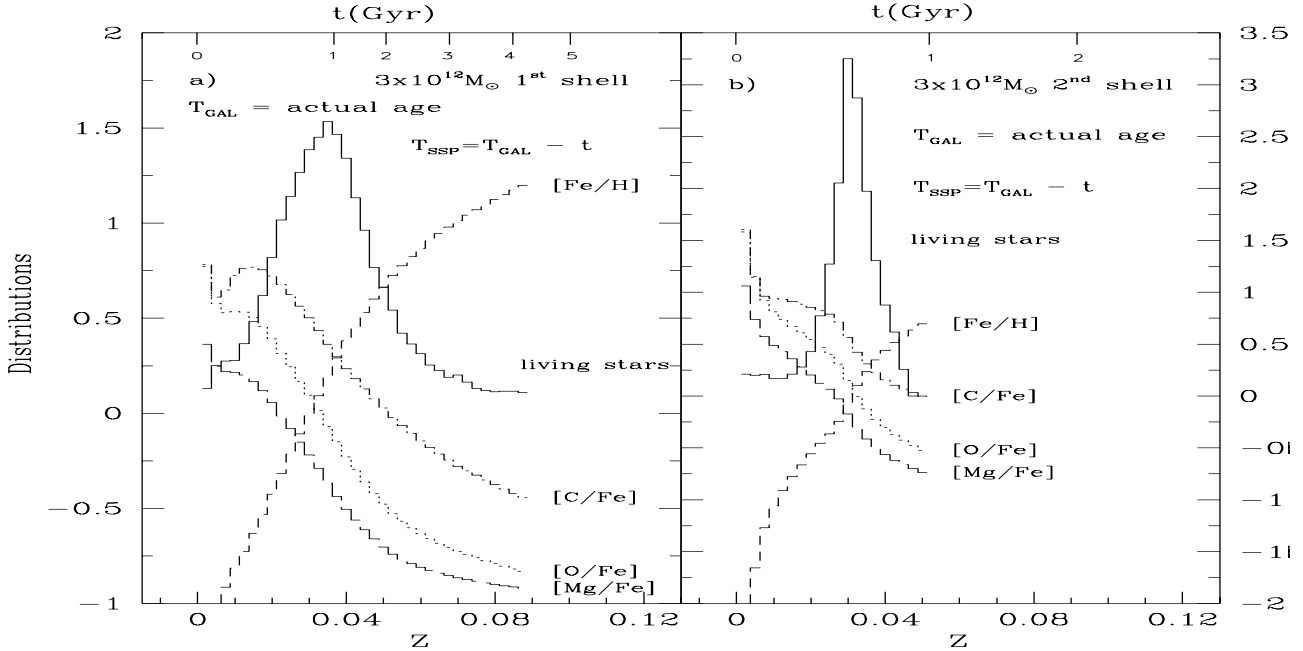


**Fig. 3.** Panels (a) and (b): the number of living stars and abundance ratio distribution per metallicity bin in the central core and the 1<sup>st</sup> shells, respectively, of the galaxy with mass  $3M_{L,12}$ . The abundance ratios are in the standard notation. The *solid line* is distribution of living stars in units of  $10^{11} M_{\odot}$ . The *dotted, dashed, long-dashed, and dot-dashed* lines give the distribution per metallicity bin of  $[O/Fe]$ ,  $[Fe/H]$ ,  $[Mg/Fe]$ , and  $[C/Fe]$ , respectively. The top scale gives the birth-time  $t = T_G - T_{SSP}$  in Gyr of a SSP of age  $T_{SSP}$  in a galaxy of age  $T_G$

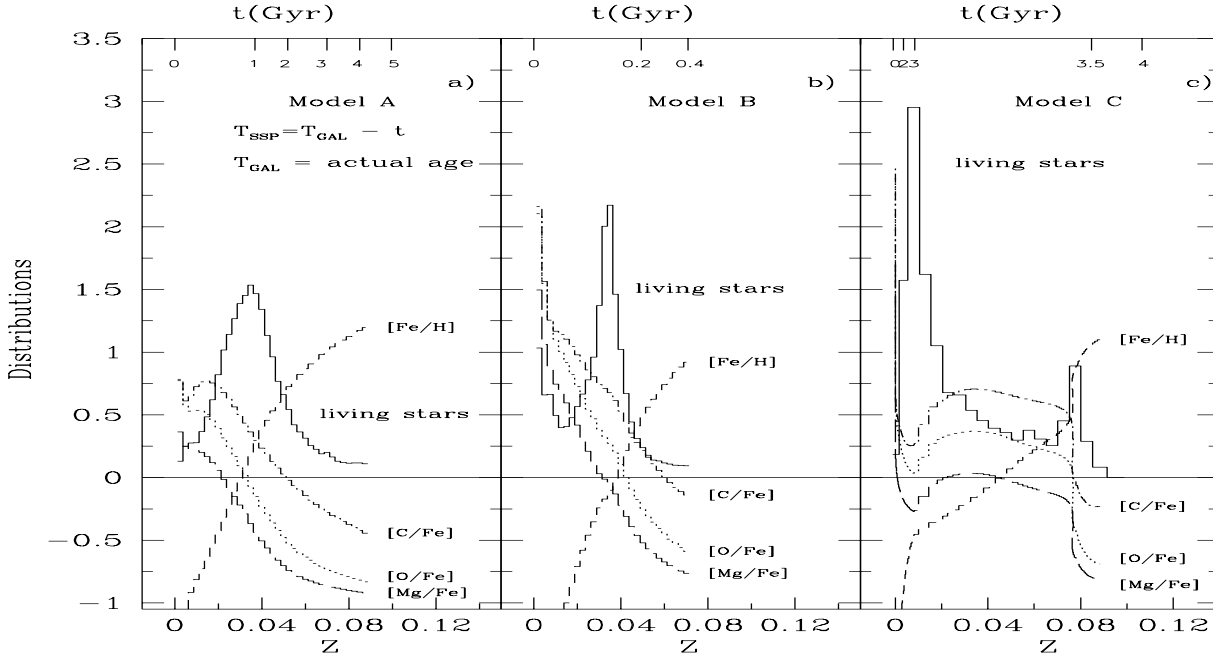


**Fig. 6.** The partition function  $N(Z)$  and abundance ratios distribution per metallicity bin, for the Model-A (left panel), Model-B (middle panel), and Model-C (right panel). The *solid line* is  $N(Z)$  in units of  $10^{11}$  at the age of 15 Gyr. The *dotted*, *dashed*, *long-dashed*, and *dot-dashed* lines give the distribution per metallicity bin for  $[O/Fe]$ ,  $[Fe/H]$ ,  $[Mg/Fe]$  and  $[C/Fe]$ , respectively. The abundance ratios are in the standard notation. The top scale gives the birth-time  $t = T_G - T_{SSP}$  of a SSP with age  $T_{SSP}$  in a galaxy with age  $T_G$

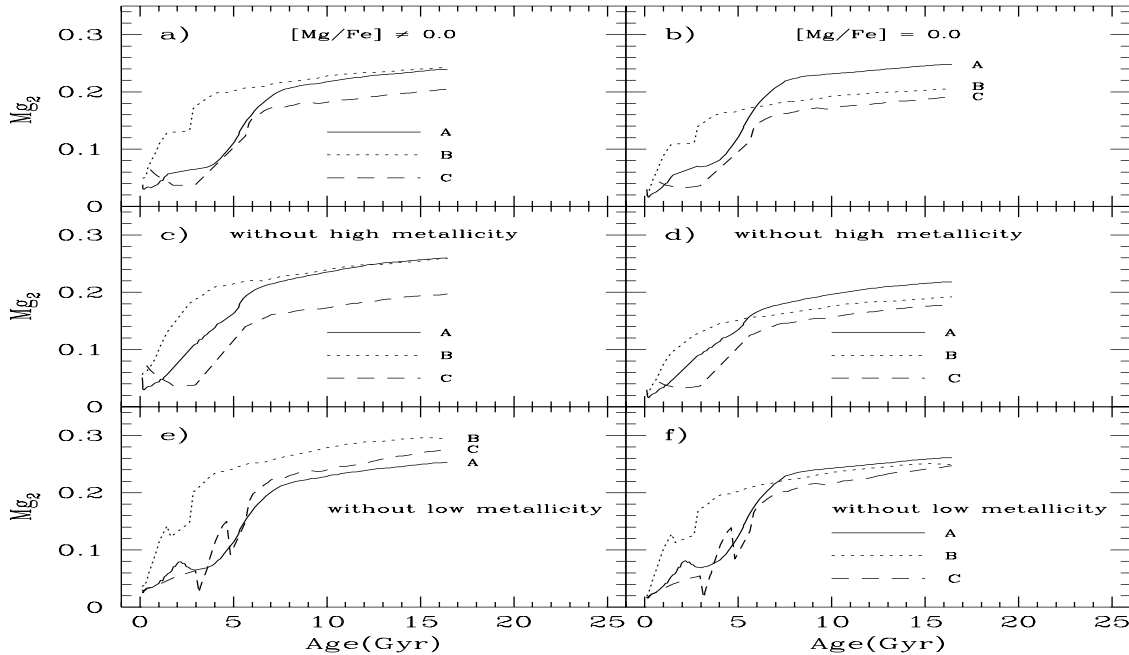


**Fig. 9.** Evolution of the  $Mg_2$  index as a function of time. *Panels (a), (c) and (e)* show the evolution of the  $Mg_2$  index calculated including the effect of the chemical abundances, while *Panels (b), (d) and (f)* show the same but without the effect of  $\alpha$ -enhancement. The *solid line* corresponds to Model-A the *dotted line* to Model-B, and *dashed line* to Model-C

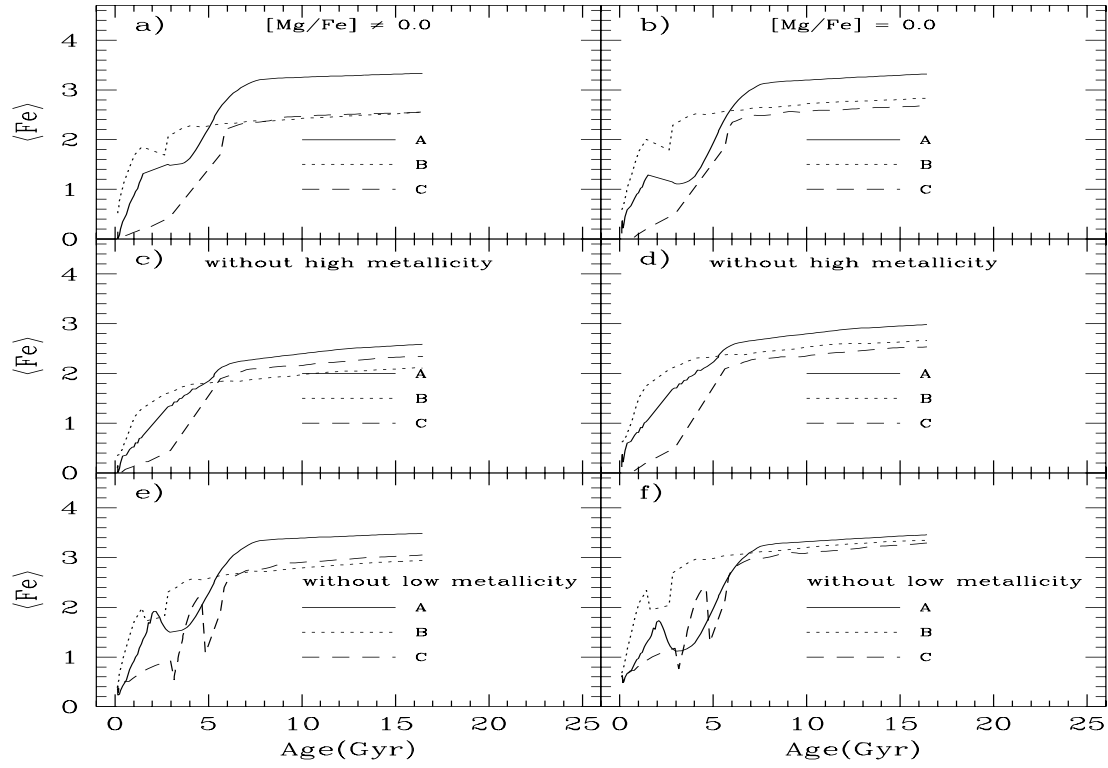


**Fig. 10.** Evolution of the  $\langle Fe \rangle$  index as a function of time. *Panels (a), (c) and (e)* show the evolution of the  $Mg_2$  index calculated including the effect of the chemical abundances, while *Panels (b), (d) and (f)* show the same but without the effect of  $\alpha$ -enhancement. The *solid line* corresponds to Model-A the *dotted line* to Model-B and *dashed line* to Model-C